Journal of Nuclear Materials 378 (2008) 153–158

Contents lists available at ScienceDirect

Journal of Nuclear Materials

journal homepage: www.elsevier.com/locate/jnucmat

M_2N nitride phases of 9% chromium steels for nuclear applications

Y.Z. Shen *, S.H. Kim, H.D. Cho, C.H. Han, W.S. Ryu, C.B. Lee

Nuclear Materials Research Center, Korea Atomic Energy Research Institute, 1045 Daedeok-daero, Yuseong, Daejeon 305-353, Republic of Korea

ARTICLE INFO

Article history:
Received 17 November 2007
Accepted 30 April 2008

PACS:
28.52.Fa
75.50.Bb
81.05.Je

ABSTRACT

M_2N nitride phases of 9% chromium steels with an extra-low carbon content have been investigated using a transmission electron microscope and an energy-dispersive X-ray (EDX) spectroscopy. The steel samples were normalized for 1 h at 1050 °C and then tempered at 600–780 °C for 30 min to 5 h followed by an air cooling. Through the analyses of the electron micro-diffraction patterns and EDX data for the precipitate particles on the extracted carbon replica, two types of Cr-rich M_2N nitride phases with the same hexagonal structure but totally different lattice parameters, a = 2.80 Å/c = 4.45 Å and a = 7.76 Å/c = 4.438 Å, were determined in the steels. Four types of Cr-rich M_2N phases with different lattice parameters probably existed in the steels. The M_2N phase revealed a decrease in its Cr content, an increase in its V content as the tempering temperature was increased, and no obvious change in its content for the metal fraction with an increasing tempering time.

1. Introduction

The 9 and 12% chromium transformable (ferritic/martensitic) steels with lower carbon (0.1% max) contents and additions of Mo, W, V, Nb, N and other elements, possessing a higher thermal conductivity, lower thermal expansion, higher resistance to a radiation embrittlement and swelling, and higher creep-rupture strengths combined with a good oxidation and corrosion resistance at elevated temperatures, have subsequently been developed. These steels have been considered for use as nuclear fission and fusion reactor components [1–4]. These ferritic steels are commonly used in a 'normalized and tempered' condition. In commercial practice, the normalized steels, which consist of a typical martensite lath network microstructure, are tempered by a heating between 650 to 780 °C. Tempered 9 and 12%Cr steels consist of a ferritic matrix with primary precipitates, $M_{23}C_6$, and small amounts of MC, and M_2X have been reported in some cases [5]. The precipitation of secondary phases and the development of a matrix in a steel during a tempering will determine the properties of that steels [6]. M_2X and secondary MX phases occur as fine particles, uniformly distributed throughout a matrix, and initially they contribute to the creep strength of that material by acting as barriers to dislocation movement at high temperatures, i.e., classical precipitation strengthening [7].

To avoid the formation of a large-sized $M_{23}C_6$ precipitation in conversional 9%Cr steels and to promote the formation of fine MX carbonitrides along the lath, block, packet and prior austenite grain boundaries as well as in the matrix during a tempering, an extremely low carbon (0.002 wt%) 9%Cr steel has been developed and proven to have a significant improvement in its creep resistance [8–9].

The suppression of a void swelling, which occurs under a high flux irradiation, is one of the most important problems for the materials that will be used in fast breeder reactors and fusion reactors. In general, it is necessary for a void formation to form a supersaturation of vacancies and or a preferential sink for self-interstitials [10]. Effect of a precipitation on a void formation can be considered in many processes. Closely spaced second-phase particles, such coherent gamma-prime ($Ni_3(Al,Ti)$) precipitates in nickel alloys and $Ti_5(Si,P)_3$ precipitates in vanadium alloys, lower the overall point defect concentration by providing sites for a mutual annihilation of vacancies and interstitials such that large excess vacancy concentrations do not occur, and a nucleation as well as a growth of voids is inhibited [11–12]. In the case of Fe–Cr and Fe–Cr–Si alloys, small precipitates will act as void nucleation sites due to the interaction process between point defects and a particle–matrix interface [13]. Void swelling for a Cu–Fe alloy containing many fine coherent precipitates would be suppressed by a mutual annihilation of its precipitates [10]. For austenitic steels, the dispersion of fine MC and M_6C precipitates reduces their void swelling and improves their resistance to a helium embrittlement, however, a coarsening of their coarser phases like the $M_{23}C_6$, M_6C, Laves, and G phases causes an accumulation of the point defect at a precipitate–matrix interface and leads to a channel formation to the attached voids [14–17].

The M_2X phase which is initially based on $Cr_2(CN)$, has a hexagonal structure and mainly nucleates on the dislocations in a tempered martensite matrix. M_2X has the following orientation relationship with the matrix formed during a tempering:

* Corresponding author. Tel.: +82 42 868 2493; fax: +82 42 868 8549.
E-mail address: shenliu8@snu.ac.kr (Y.Z. Shen).

0022-3115/$ - see front matter © 2008 Elsevier B.V. All rights reserved.
doi:10.1016/j.jnucmat.2008.04.020

$(0001)_{M2X}//(011)_{\alpha}$ and $[1120]_{M2X}//[100]_{\alpha}$ [18]. Fine M_2N precipitate particles were also observed to be present and uniformly dispersed throughout the matrix of high Cr steels [7]. It is expected that the void swelling resistance of ferritic steels during an irradiation at an elevated temperature can be partially attributed to the presence of fine coherent Cr-rich M_2X nitride particles.

A microstructural investigation of the alloy carbides and nitrides for high Cr steels is important to understand their creep properties and void swelling resistance. We have already reported on the presence of vanadium-rich MN precipitate phases in an extra-low carbon 9%Cr steel [19]. In this paper, results for the presence of M_2N nitride precipitate phases in extra-low carbon 9%Cr steels investigated by TEM (transmission electron microscope) and EDX (energy-dispersive X-ray) analysis are reported.

2. Experimental procedure

Two high-chromium ferritic steels prepared by a melting, casting and hot rolling were used in this investigation. The chemical compositions (in wt%) of the steels were <0.003 C, 9.88 Cr, 1.20 Mo, 0.20 V, 0.20 Nb, 0.43 Mn, 0.37 Ni, 0.105 Si, 0.084 N (named after L) and <0.003 C, 9.88 Cr, 0.51 Mo, 2.09 W, 0.20 V, 0.20 Nb, 0.43 Mn, 0.37 Ni, 0.105 Si, 0.084 N (named after LW).

Hot-rolled steel plate samples of 15 mm in thickness underwent a normalization heat treatment at 1050 °C for 1 h, and then a tempering at 600, 650, 700, 750 and 780 °C for 2 h, and they were named L43/LW43, L44/LW44, L45/LW45, L46/LW46 and L47/LW47, respectively. Tempering was also performed for 30 min, 1 h, and 5 h at 750 °C for the LW steel samples. All the steel samples were cooled in air at room temperature after the heat treatments.

Extracted carbon replicas were prepared by the evaporation of carbon onto a polished and etched steel sample surface followed by a dissolution of the metallic matrix in a solution of 10%HCl–methanol at a voltage of 2 V at 20 °C.

Extracted carbon replicas were examined using a JEM-2000 FXII TEM equipped with a LINK EDX system and operating at a 200 kV accelerating voltage. The compositions of the precipitate phases were detected by EDX analysis. Precipitate phases were identified by a combination of the micro-diffraction (MD) pattern and EDX analysis results.

3. Results and discussion

Fig. 1 shows the TEM images of the LW44 steel taken from a replica sample and the MD patterns taken from the precipitate 1

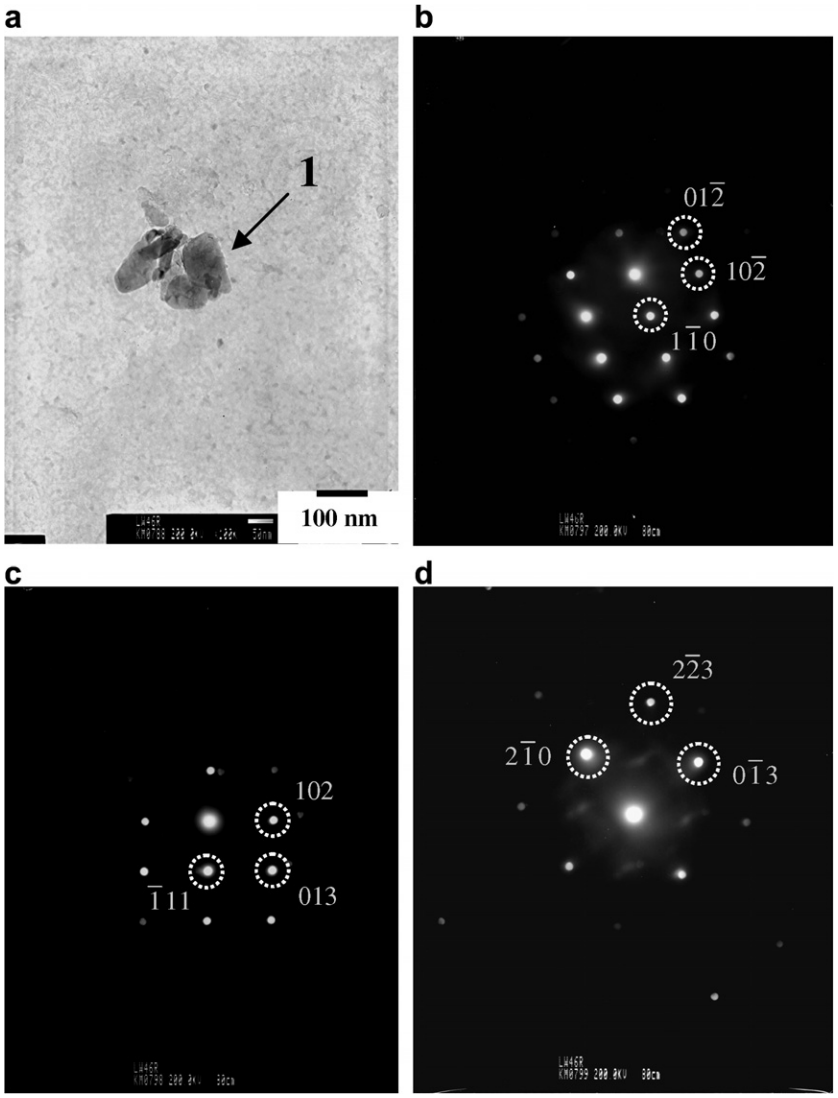

Fig. 1. TEM micrograph (a) of the LW44 steel taken from a carbon replica, showing M_2N precipitate 1, and the micro-diffraction patterns taken from precipitate 1 in the three zone axes of (b) [223], (c) $[14\bar{3}]$ and (d) [032].

Table 1
Matching the diffraction patterns of the M_2N precipitate taken from the 9%Cr steels with that of the Cr_2N phase from the JCPDS file and various references

Sample	Pattern	Cr_2N phase (hexagonal)			EDX analysis result (in at.%) (precipitate particle)
		a = 2.80[a] c = 4.45[b] Ref. [5]	a = 4.78 c = 4.44 01-1232[c]	a = 7.76 c = 4.438 Ref. [18]	
LW44	Fig. 1(b)	[2 2 3][d] ΔR = 0.017[e] $\Delta\theta$ = 0.7°[f]	[0 2 3] ΔR = 0.027 $\Delta\theta$ = 0.4°	[3 1 8] ΔR = 0.066 $\Delta\theta$ = 3.0°	92.1Cr–2.3V–0.9Nb–0.9Mo–2.6W–1.2Fe (precipitate 1)
	Fig. 1(c)	[1 4 $\bar{3}$] ΔR = 0.026 $\Delta\theta$ = 1.3°	No matching	[3 2 5] ΔR = 0.046 $\Delta\theta$ = 2.4°	
	Fig. 1(d)	[0 3 2] ΔR = 0.051 $\Delta\theta$ = 1.2°	No matching	No matching	
LW46	Fig. 2(b)	No matching	No matching	[0 1 0] ΔR = 0.082 $\Delta\theta$ = 1.8°	79.2Cr–17.3V–0.9Mo–0.7W–1.9Fe (precipitate 2)
L46	Fig. 2(d)	No matching	No matching	[0 1 0] ΔR = 0.095 $\Delta\theta$ = 1.6°	82.8Cr–14.2V–1.0Nb–1.6Mo–0.4Fe (precipitate 3)
LW43	Fig. 3(b) Fig. 3(c)	[1 1 3] ΔR = 0.052 $\Delta\theta$ = 1.0°	[0 2 1] ΔR = 0.052 $\Delta\theta$ = 2.1°	No matching	92.0Cr–3.9V–1.4Mo–2.2W–0.5Fe (precipitate 4)
L43	Fig. 4(b)	No matching	No matching	No matching	88.6Cr–5.0V–6.4Mo (precipitate 5)

[a,b] Lattice parameter, Å.
[c] JCPDS file.
[d] Zone axis, [UVW], i.e., incident beam direction.
[e] The maximum error range in the distance of diffraction sport from origin when matched diffraction pattern obtained with the data from Cr_2N phase, mm.
[f] The maximum error range in the angles between crystal planes P_1 and P_2 or P_1 and P_3 when matched diffraction pattern obtained with the data from Cr_2N phase.

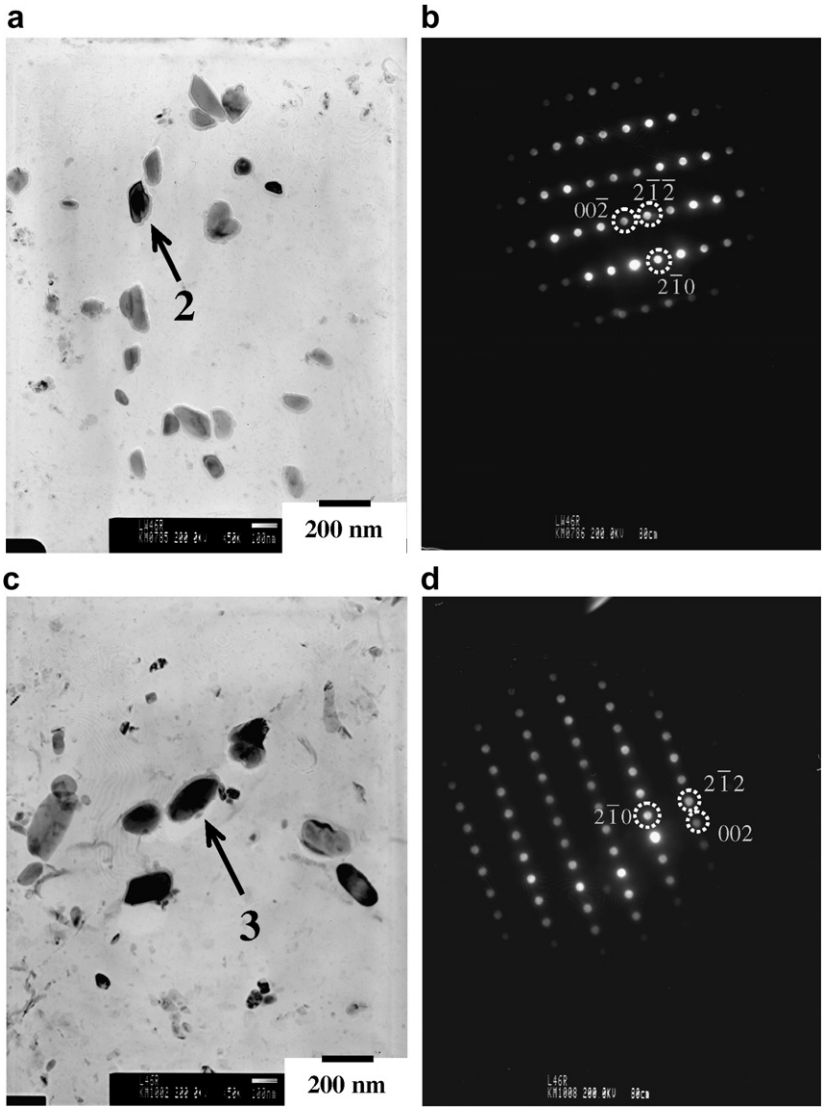

Fig. 2. TEM micrographs (a) and (c) of the LW46 and L46 steels taken from a carbon replica, showing M_2N precipitate 2 and 3, respectively, and the micro-diffraction patterns taken from precipitate 2 and 3 in the same zone axis of [0 1 0].

marked with an arrow. The EDX analysis result of the precipitate 1 indicates that the precipitate is a chromium-rich nitride phase and has a chemical composition of 92.1Cr–2.3V–0.9Nb–0.9Mo–2.6W–1.2Fe (in at.%), as given in Table 1. All three MD patterns in Fig. 1(b)–(d) match well with the electron diffraction patterns from chromium nitride (Cr_2N) with a hexagonal crystal structure and lattice parameters of $a = 2.80$ Å, $c = 4.45$ Å from reference [5] in the three zone axes of [223], [$14\bar{3}$] and [032], respectively. Since only one (Fig. 1(b)) or two (Fig. 1(b) and Fig. 1(c)) of the three MD patterns recorded from precipitate 1 could be or seem to be matched with the diffraction patterns from the hexagonal Cr_2N phase with lattice parameters of $a = 4.78$ Å, $c = 4.44$ Å (JCPDS file 01-1232)/or $a = 7.76$ Å, $c = 4.438$ Å [20] in the zone axes of [023]/ or [318] and [325], respectively. Therefore, precipitate 1 does not belong to the Cr_2N with lattice parameters of $a = 4.78$ Å, $c = 4.44$ Å and the Cr_2N with the lattice parameters of $a = 7.76$ Å and $c = 4.438$ Å.

Figs. 2(a) and (c) present the TEM images of the LW46 and L46 steels taken from the replica samples, revealing a chromium-rich nitride precipitate 2 and 3. The chemical composition (in at.%) is 79.2Cr–17.3V–0.9Mo–0.7W–1.9Fe for precipitate 2 and 82.8Cr–14.2V–1.0Nb–1.6Mo–0.4Fe for precipitate 3, as listed in Table 1. The MD patterns taken from precipitates 2 and 3 are shown in Fig. 2(b) and (d), respectively, which match well with the electron diffraction patterns from chromium nitride (Cr_2N) with lattice parameters of $a = 7.76$ Å, $c = 4.438$ Å from Ref. [20] in the same zone axis of [010]. Thus, the observed chromium-rich nitride precipitates are M_2N phases and have lattice parameters of $a = 7.76$ Å and $c = 4.438$ Å, but do not $a = 2.80$ Å and $c = 4.45$ Å or $a = 4.78$ Å and $c = 4.44$ Å because these two MD patterns could not be correlated with any diffraction patterns from the Cr_2N phases (Ref. [5] and JCPDS file 01-1232).

Fig. 3(a) is the TEM micrograph of the LW43 steel taken from a replica sample, revealing a chromium-rich nitride precipitate 4 with a chemical composition of 92.0Cr–3.9V–1.4Mo–2.2W–0.5Fe (in at.%). One MD pattern, Fig. 4(b) or (c), was taken from precipitate 4. The pattern could not be correlated with the diffraction pattern from Cr_2N with lattice parameters of $a = 7.76$ Å and $c = 4.438$ Å from Ref. [20] in any zone axis, whereas it matched well with the diffraction pattern, within the maximum error range for a distance

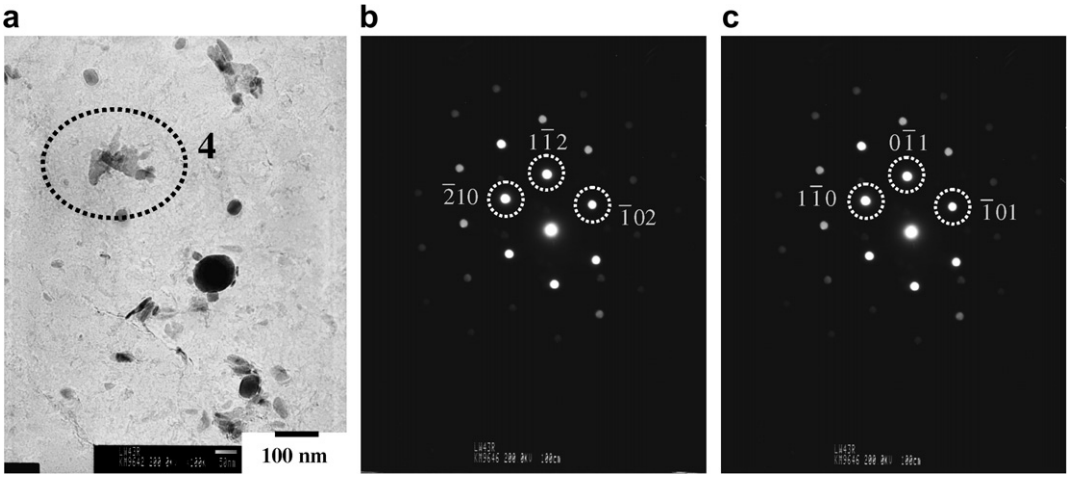

Fig. 3. TEM micrograph (a) of the LW43 steel taken from a carbon replica, showing M_2N precipitate 4, and the micro-diffraction patterns taken from precipitate 4 and indexed according to the two zone axes of (b) [021] and (c) [113].

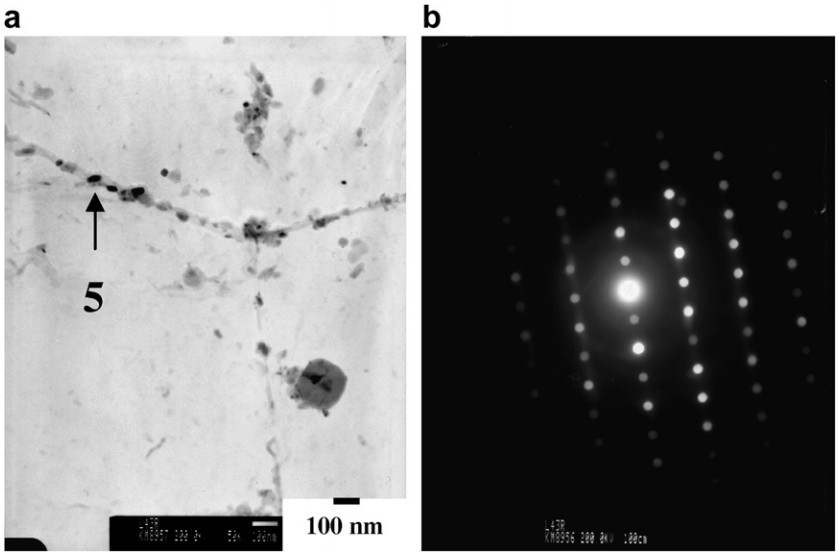

Fig. 4. TEM micrograph (a) of the L43 steel taken from a carbon replica, showing M_2N precipitate 5, and the micro-diffraction pattern (b) taken from the precipitate 5.

and angle of $\Delta R = 0.049$ mm/$\Delta\theta = 1.0°$ or $\Delta R = 0.052$ mm/$\Delta\theta = 2.1°$ (Table 1) from Cr_2N with lattice parameters of $a = 2.80$ Å and $c = 4.45$ Å [5] or $a = 4.78$ Å and $c = 4.44$ Å (JCPDS file 01-1232) in the zone axis of [1 1 3] or [0 2 1], respectively. As a result, the lattice parameters of the Cr-rich M_2N precipitate 4 should be $a = 2.80$ Å and $c = 4.45$ Å or $a = 4.78$ Å and $c = 4.44$ Å, but not $a = 7.76$ Å and $c = 4.438$ Å, indicating that there is a possibility for the presence of a M_2N phase with lattice parameters $a = 4.78$ Å and $c = 4.44$ Å from the JCPDS file 01-1232 in the 9%Cr steel.

Fig. 4 shows one TEM image and one MD pattern taken from a carbon replica of the L43 steel. The chemical composition of precipitate 5 was 88.6Cr–5.0V–6.4Mo (in at.%) which was determined through an EDX analysis. We tried to index this MD pattern according to three kinds of Cr_2N phases listed in Table 1, but there is no probable diffraction pattern to match the MD pattern of precipitate 5. In consideration of the EDX result for precipitate 5, the possible Cr-rich precipitates containing nitrogen in high Cr steels except for the three Cr_2N phases given in Table 1 could be other Cr_2N (Hexagonal, lattice parameters of $a = 4.805/4.8113$ Å, $c = 4.479/4.484$ Å, JCPDS file 27-0127/35-0803), CrN (fcc, $a = 4.14$ Å, 11-0065), $(Cr,Mo)_2(C,N)$ (hexagonal, $a = 2.89$ Å, $c = 4.56$ Å, 08-0270), $(Cr,Fe)_2N_{1-x}$ (hexagonal, $a = 4.8$ Å, $c = 4.462$ Å, 19-0330), $Cr_2N_{0.39}C_{0.61}$ (ortho, face, C, $a = 4.883$ Å, $b = 5.599$ Å, $c = 4.438$ Å, 19-0325). Pattern-indexing results indicate that the MD pattern of precipitate 5 could not be matched with a diffraction pattern from the phases mentioned above for any zone axis even in the maximum error range for the angle between the crystal planes when matched the MD pattern with the indexing data from those phases was $\Delta\theta = 5°$. From the EDX data, the observed Cr-rich nitride is probably a Cr_2N phase containing molybdenum, vanadium and niobium, and also a hexagonal structure but with its lattice constants of the *a*-axis and *c*-axis considerably different from the lattice parameters of the Cr_2N phases mentioned in this paper, which should be verified by further experimental work and calculations.

The structures and lattice parameters of the Cr_2N phase have been reported as the following types: hexagonal with $a = 2.80/2.8$ Å, $c = 4.45/4.4$ Å [5]/[21]; hcp with $a = 2.748$ Å, $c = 4.438$ Å [22]; hcp with $a = 7.76$ Å, $c = 4.438$ Å [20]; hexagonal with $a = 4.78/4.685$ Å, $c = 4.44/4.306$ Å (JCPDS 01-1232)/[23]; trigonal with $a = 4.752(3)/4.800(4)$ Å, $c = 4.429(4)/4.472(5)$ Å [24]/[25]. It can be seen that there is no large difference between the *c*-axis lattice constants, and one can roughly divide the *a*-axis lattice constants into three types, i.e., $a = 2.78$, 4.75, and 7.76 Å. We have determined that two types of Cr_2N (Cr-rich nitride) phases with *a*-axis lattice constants of 2.80 and 7.76 Å existed in the present 9%Cr steels. Cr_2N (Cr-rich nitride) phase with an *a*-axis lattice constant of about 4.75 Å is a possible phase existed in the present 9%Cr steels. It is possible that there is a Cr_2N (Cr-rich nitride) phase with lattice constants considerably different from the three mentioned above, regarding precipitate 5 shown in Fig. 4.

Figs. 5 and 6 present the alloying element content of the M_2N precipitate phase in the present 9%Cr steels as a function of the tempering temperature and time, respectively. With an increasing tempering temperature for the tempering time of 2 h, the vanadium content increased, whereas the chromium content decreased, and there was no obvious change in the contents of the other elements such as molybdenum, tungsten and iron. This result is strikingly different from a reported result that the contents of Cr and Fe, and Mo in a M_2X phase increased and decreased as the tempering temperature was increased from 600 to 700 °C and 750 °C, respectively [6]. It has also been reported that the molybdenum content of a M_2C carbide was increased obviously, while the contents of Cr and Fe were decreased when the tempering time at 700 °C was increased [26]. However, in the present case, no obvious change in the contents of all the metallic elements in the M_2N phase was found as the tempering time was increased at 750 °C.

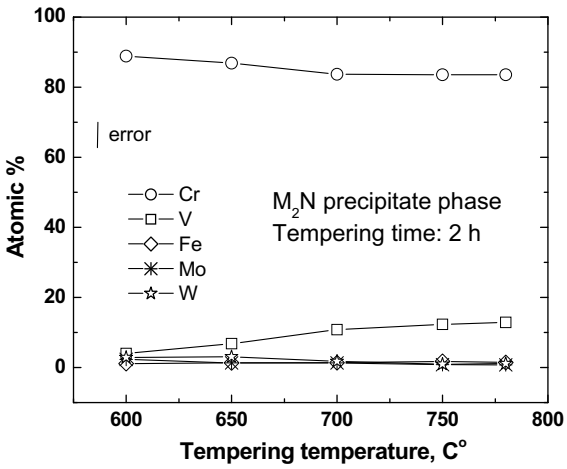

Fig. 5. The content of the metallic elements in the M_2N nitride phase as a function of the tempering temperature in the 9% Cr steels.

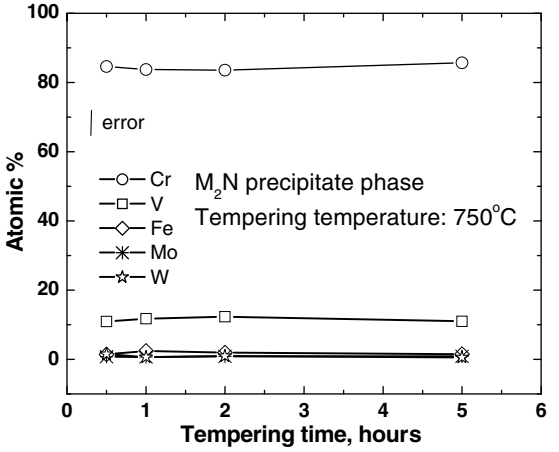

Fig. 6. The content of the metallic elements in the M_2N nitride phase as a function of the tempering time in the 9% Cr steels.

4. Conclusions

This study on the M_2N precipitate phase in extra-low carbon 9% chromium steels with tempered conditions has indicated that two types of Cr-rich M_2N precipitate phases with the same hexagonal structure but different lattice parameters, $a = 2.80$ Å/$c = 4.45$ Å and $a = 7.76$ Å/$c = 4.438$ Å, coexisted in the steels, and four types of Cr-rich M_2N phases probably existed in the steels. The Cr-rich nitride M_2N revealed a decrease in its chromium content, an increase in its vanadium content as the tempering temperature was increased, and no obvious change in its composition for the metal fraction with an increasing tempering time.

Acknowledgements

This study has been supported by Korea Science and Engineering Foundation (KOSEF) and Ministry of Science & Technology (MOST), Korean government, through its Mid and Long-Term Nuclear R&D Plans.

References

[1] R.L. Klueh, D.R. Harries, High-Chromium Ferritic and Martensitic Steels for Nuclear Applications, ASTM, West Conshohocken, PA, 2001.
[2] F. Abe, T. Noda, H. Araki, M. Okada, J. Nucl. Sci. Technol. 31 (1994) 279.

[3] S.N. Rosenwasser, P. Milier, J.A. Dalessandro, J.M. Rawls, W.E. Toffolo, W. Chen, J. Nucl. Mater. 85&86 (1979) 177.
[4] D.S. Gelles, ISIJ Int. 30 (1990) 905.
[5] J.M. Vitek, R.L. Klueh, Mater. Trans. A 14 (1983) 1047.
[6] G.J. Cai, H.O. Andrén, F.L.E. Svensson, Mater. Sci. Eng. A 242 (1998) 202.
[7] A. Strang, V. Vodárek, in: A. Strang, D.J. Gooch (Eds.), Microstructural Development and Stability in High Chromium Ferritic Power Plant Steels, The Institute of Materials, London, 1997, p. 31.
[8] M. Taneike, F. Abe, K. Sawada, Nature 424 (2003) 294.
[9] K. Sawada, M. Taneike, K. Kimura, F. Abe, ISIJ Int. 44 (2004) 1243.
[10] T. Takeyama, S. Ohnuki, H. Takahashi, J. Nucl. Mater. 89 (1980) 253.
[11] W.K. Appleby, D.W. Sandusky, U.E. Wolff, J. Nucl. Mater. 43 (1972) 213.
[12] H.M. Chung, D.L. Smith, J. Nucl. Mater. 191–194 (1992) 942.
[13] S. Ohnuki, H. Takahashi, T. Takeyama, J. Nucl. Mater. 122&123 (1984) 317.
[14] T. Kimoto, H. Shiraishi, J. Nucl. Mater. 141–143 (1986) 754.
[15] S. Ukai, T. Uwaba, J. Nucl. Mater. 317 (2003) 93.
[16] P.J. Maziasz, J. Nucl. Mater. 122&123 (1984) 472.
[17] A.D. Brailsford, R. Bullough, J. Nucl. Mater. 44 (1972) 121.
[18] F.B. Pickering, in: A. Strang, D.J. Gooch (Eds.), Microstructural Development and Stability in High Chromium Ferritic Power Plant Steels, The Institute of Materials, London, 1997, p. 1.
[19] Y.Z. Shen, S.H. Kim, C.H. Han, H.D. Cho, W.S. Ryu, C.B. Lee, J. Nucl. Mater. 374 (2008) 403.
[20] A. Runiewicz, W. Dudzinski, A. Fischer, Prakt. Metallogr. 43 (2006) 364.
[21] H. Era, Y. Ide, A. Nino, K. Kishitake, Surf. Coat. Technol. 194 (2005) 265.
[22] P.H. Mayrhofer, F. Rovere, M. Moser, C. Strondl, R. Tietema, Scripta Mater. 57 (2007) 249.
[23] A. Toro, W.Z. Misiolek, A.P. Tschiptschin, Acta Mater. 51 (2003) 3363.
[24] S.J. Kim, T. Marouart, H.F. Franzen, Less Common Metals 158 (1990) L9.
[25] T.H. Lee, S.J. Kim, E. Shin, S. Takaki, Acta Crystallogr. 62 (2006) 979.
[26] J. Pilling, N. Ridley, Mater. Trans. A 13 (1982) 557.